# A UHF Frontend for MIMO Applications in RFID

Robert Langwieser, Christoph Angerer, and Arpad L. Scholtz

Institute of Communications and Radio-Frequency Engineering
Vienna University of Technology, Austria
email: {rlang, cangerer, ascholtz}@nt.tuwien.ac.at

***Abstract*— The introduction of multi antenna applications in radio frequency identification (RFID) is expected to further improve the capability of RFID systems but requires new or extended simulation and experimental setups. This paper describes a developed analog $2 \times 2$ multiple input multiple output (MIMO) frontend for an RFID rapid prototyping system which allows for various realtime experiments to investigate MIMO techniques as beamforming, diversity combining, or localization at the reader. Finally, a measurement example with one transmitter and two receivers is presented for two different tag positions.**

***Index Terms*— frontend, MIMO, rapid prototyping, reader, RFID, UHF.**

## I. Introduction

The combination of radio frequency identification (RFID) and sensor technologies opens a new area of applications [1]. To meet the requirements for these new applications a performance increase of current RFID systems is desired [2]. The use of advanced multi antenna transmit and receive techniques like beamforming, spatial multiplexing, or diversity combining at the reader is expected to improve the reader performance and therefore also the whole system performance significantly [3]-[5].

To enable experimental research concerning multiple input multiple output (MIMO) techniques in RFID we have implemented an analog $2 \times 2$ (2 transmitters $\times$ 2 receivers) MIMO frontend, supporting the European ultra high frequency (UHF) band from 865 MHz to 868 MHz. The frontend is operated as part of an RFID rapid prototyping system. This experimental environment allows to analyze interdependencies of system parameters like backscatter link frequency (BLF), packet errors, throughput, signal to noise ratio (SNR), transmit power, carrier interference, and different frontend and antenna configurations. Additionally, it allows for fast testing of novel and non standard compliant implementations [6].

In Section II we describe the overall hardware concept of our rapid prototyping system. The investigated MIMO frontend is described in Section III. A measurement example with a system of one transmitter and two receivers is given in Section IV. This example shows the good performance of the frontend as part of the experimental setup. Finally, in Section V we conclude and summarize our paper.

This work has been funded by the Christian Doppler Laboratory for Wireless Technologies for Sustainable Mobility. Furthermore, our industrial partner Infineon Technologies has to be thanked for enabling this work.

## II. Hardware Concept for Rapid Prototyping

The setup of a rapid prototyping system requires a lot of high quality resources which typically would not be used for commercial products. Therefore it provides much more flexibility and insight into functionality and raw performance than commercially available readers. Rapid prototyping is used to evaluate functionality and performance of novel and crucial technologies on hardware at an early design stage. The hardware of a rapid prototyping environment can be divided into three system parts:

- digital baseband
- interface between digital and analog domain
- analog frontends

On the digital baseband part the new or crucial algorithms will be implemented for evaluation under realistic conditions. Also tasks like modulation or pulse shaping are shifted into the digital domain. The core components of such a digital baseband hardware are usually programable parts like microcontrollers, digital signal processors (DSPs), field programable gate arrays (FPGAs), and memories.

The second system part consist of the interfacing components between the analog and the digital domain. These components are usually analog-to-digital converters (ADCs) and digital-to-analog converters (DACs). In most cases this part is integrated either to the digital baseband hardware or to the analog frontend part.

Finally, analog frontends are required for transmission experiments and validation (or invalidation) at radio frequencies (RF). They often are the bottleneck during the implementation of testbeds, demonstrators as well as rapid prototyping environments, especially for MIMO systems which are of higher complexity. The main tasks of the analog frontend are filtering, frequency conversion, and amplification without degrading signal quality. Especially for rapid prototyping, such frontends should be configurable and scalable to allow for a multitude of experiments

without time consuming redesigns. Fig. 1 shows our rapid prototyping hardware setup for RFID.

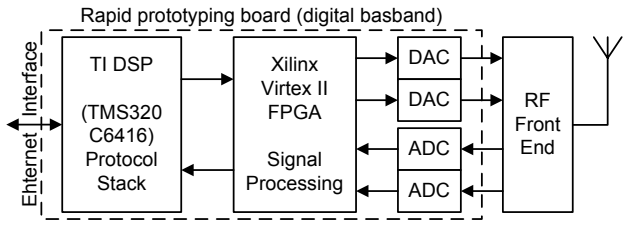


Fig. 1. Simplified block diagram of the rapid prototyping hardware setup.

- The digital baseband platform is set up with a commercially available board especially designed for rapid prototyping in the field of wireless communication [7]. The board provides a DSP which is used for the protocol issues of RFID and an FPGA which permits flexible implementation of different transmitter and receiver structures [8]. Also integrated to the rapid prototyping board are two DACs and two ADCs for interfacing the analog frontends. The interlink between the digital and analog parts can be either directly at baseband with inphase (I) and quadrature-phase (Q) signals or at a suitable low intermediate frequency.
- The analog frontends are exchangeable and designed to meet the requirements for rapid prototyping especially in the field of RFID. Currently, frontends are developed for HF at 13.56 MHz and the European UHF band from 865 MHz to 868 MHz [9].

## III. UHF MIMO Frontend Description

The frontend is basically built of two identical transmitters and two identical receivers which perform mainly frequency conversion, filtering, and amplification. The transmitters and receivers are built with components off-the-shelf only. Fig. 2 shows the simplified block diagram for the $2 \times 2$ frontend. In the upper part of Fig. 2 the two transmitters and in the lower part the two receivers are shown. The interlink frequency between the rapid prototyping board and the MIMO frontend is 13.33 MHz. The frequency conversion to and from the desired UHF band is performed in two steps. At the transmitter in a first step from 13.33 MHz to an intermediate frequency of 140 MHz and in a second step from 140 MHz to 868 MHz and at the receiver correspondingly. The required local oscillators (LOs) LO1 and LO2 are provided by standard laboratory signal generators and distributed via 4-way power dividers to the corresponding frequency conversion stages. Therefore, all transmitters and receivers have a constant phase relationship. The 3 dB bandwidth of transmitters and receivers is 8 MHz and covers the frequency range from 862.5 MHz to 870.5 MHz. Each of

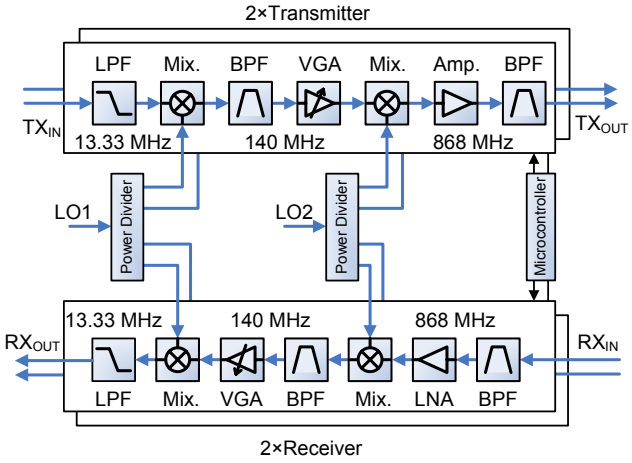


Fig. 2. UHF frontend concept for MIMO applications.

the transmitters or receivers allow amplitude adjustment via variable gain amplifiers (VGAs). These VGAs can either be controlled manually or by a microcontroller which is part of the system concept. At the transmitters gain can be varied continuously in a range of 55 dB and at the receivers digitally in a range of 40 dB with a minimum step size of 1 dB. Additionally, power monitoring at several stages of the frontend is available. The transmitters provide an output power of 20 dBm each. Therefore, short range experiments can be performed directly and the output power is sufficient to drive an external power amplifier (PA) for long range applications.

## IV. Measurement Example

Fig. 3 shows the setup with one transmitter and two receivers used for this measurement. The signal generation

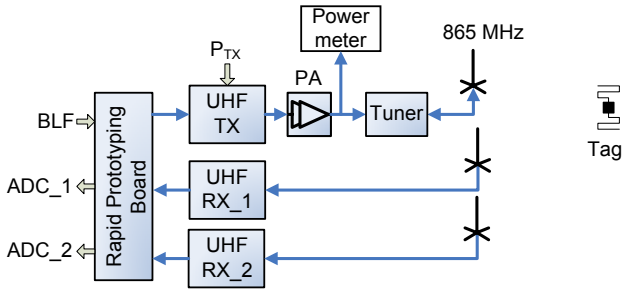


Fig. 3. Measurement setup with one transmitter and two receivers.

at the reader side is performed by the rapid prototyping board. A single query command with the continuous carrier before and after the command itself is fed after the digital-to-analog conversion at 13.33 MHz into the UHF transmitter. An external power amplifier after the transmitter is used for additional amplification of the transmit signal. After the power amplifier the transmit power is measured

using a directional coupler and a power meter. The following impedance tuner improves the antenna impedance matching.

As transmit antenna a commercially available right hand circularly polarized patch antenna with a gain of 9 dBi is used. In comparison with a linearly polarized transmit antenna with perfect polarization match with a linearly polarized tag, the power penalty at the tag caused by the polarization mismatch is 3 dB when using a circularly polarized transmit antenna and a linearly polarized tag. The advantage of the system with the circularly polarized transmit antenna is that the polarization mismatch is independent from the specific orientation of tag and reader antennas. To compensate this fixed penalty at the tag the transmit power was set to 36 dBm equivalent radiated power (ERP). This is for the tag equivalent to a transmit power 33 dBm ERP with a linearly polarized transmit antenna of equal gain and with perfect polarization match. Also at the receivers two right hand circularly polarized patch antennas are used. The gain for these antennas is 8 dBi. As for the transmit case a constant power penalty of 3 dB is introduced by the mismatch between the linearly polarized tag and the circularly polarized receive antennas but therefore again communication can not be prevented due to polarization mismatch. Both UHF receivers where adjusted for the same gain settings and the outputs at 13.33 MHz are connected to the two ADCs of the rapid prototyping board.

The measurement has been carried out indoor in a static environment. All antennas were placed in a measurement room separated from the UHF frontend and the rapid prototyping board. The connections between the antennas and the frontend were made with cables of 5 m length: Antenna TXA was connected via the impedance tuner to the power amplifier of the transmitter TX, antenna RXA_1 was connected to the receiver RX_1, and antenna RXA_2 was connected to the receiver RX_2. Fig. 4 shows the antennas – tag spatial arrangement for this measurement in a bird eye view. For this measurement two commercially available passive UHF tags were used. The tags, Tag1 and Tag2, were placed at different positions Pos.1 and Pos.2, respectively. The spatial arrangement of the transmit antenna (TXA) and the receive antennas (RXA_1 and RXA_2) has been chosen for best decoupling of transmitter and receivers. The achieved decoupling within this scenario was around 45 dB for both receivers. Two measurements were performed, one with Tag1 at Pos.1 and a second with Tag2 at Pos.2. For both measurements the same backscatter link frequency of 640 kHz was chosen. The tag (either Tag1 or Tag2) responds with its 16 bit random number after the transmitter has sent the query command. The tag answers received by both branches (RX_1 and RX_2) were sampled by the ADCs of the rapid prototyping board and stored. Both measurements were carried out with identical setups with exception of different tags and positions.

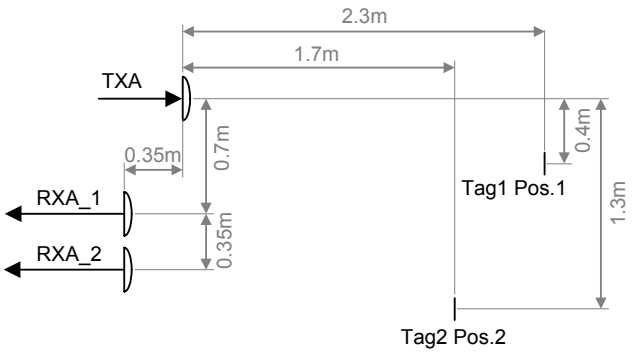


Fig. 4. Antenna and tag configuration.

Fig. 5 shows the inphase and the quadrature components of the response of tag Tag1 at position Pos.1 for both receive paths after an off-line post-processing (IQ-demodulation and filtering) of the received and stored samples. Both receive branches show comparable behavior

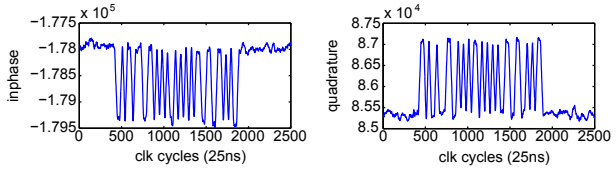


(a) Receive antenna RXA_1.

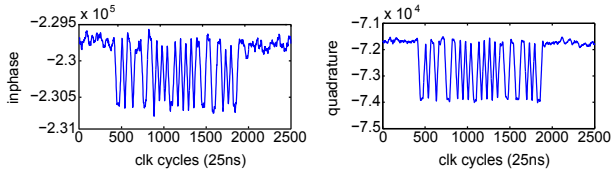


(b) Receive antenna RXA_2.

Fig. 5. Inphase and quadrature components of the response backscattered by Tag1 at position Pos.1 received by the antennas RXA_1 and RXA_2.

of the received tag answer. At the beginning, from clock cycles 0 to 400, and at the end, from clock cycle 1900 to 2500, the unmodulated carrier can be identified. This unmodulated carrier signal is dominated by the crosstalk directly from the transmit antenna to the receive antennas. The clock cycles of 25 ns corresponds to the DAC and ADCs update rate of 40 MHz. In the middle, from clock cycles 400 to 1900, the superposition of the leaking carrier and the backscatter signal caused by the change of the reflections behavior of the tag can be observed. Fig. 6 depicts the corresponding scatter plot for antenna RXA_1 and Fig. 7 shows the combination of the received constellation for the different positions Pos.1 and Pos.2 and the two receive antennas RXA_1 and RXA_2. In Fig. 6 the positions of the two constellation points of the response

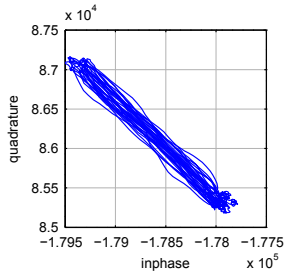


Fig. 6. Scatter plot of the tag response received by antenna RXA_1 for Tag1 at position Pos.1.

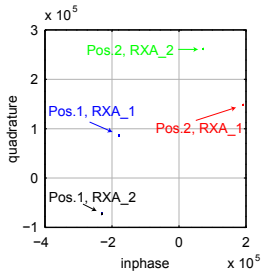


Fig. 7. Combined scatter plot for the different receive branches and the different tag positions.

can be clearly seen whereas in Fig. 7 with the different received constellations from different receive antennas and different tag positions the cross talk from the transmitter to the receivers dominates. The offset of each receive antenna–position combination represent the continuous carriers which have different amplitudes and phases in all measurements. The resulting signal to interference ratios (SIRs) of the received answers serves as a measure for the decoupling of transmitter and receivers. The signal to interference ratios at the receiver branches RX_1, RXA_1 and RX_2, RXA_2 with the tag at position Pos.1 are about $\mathrm{SIR}_1 = -38.5\,\mathrm{dB}$ and $\mathrm{SIR}_2 = -39.8\,\mathrm{dB}$, respectively. For the second scenario with tag position Pos.2 the signal to interference ratios are $\mathrm{SIR}_1 = -45.6\,\mathrm{dB}$ for the first receive path RX_1, RXA_1 and $\mathrm{SIR}_2 = -42.5\,\mathrm{dB}$ for the second receive path RX_2, RXA_2. The SIR values results from the antenna configuration and tag position used. These values are of interest for analog frontend development as well as for the minimum required dynamic range of ADCs used for sampling.

Fig. 8 shows the same combined scatter plot than Fig. 7 just without the carriers. Subtracting the corresponding

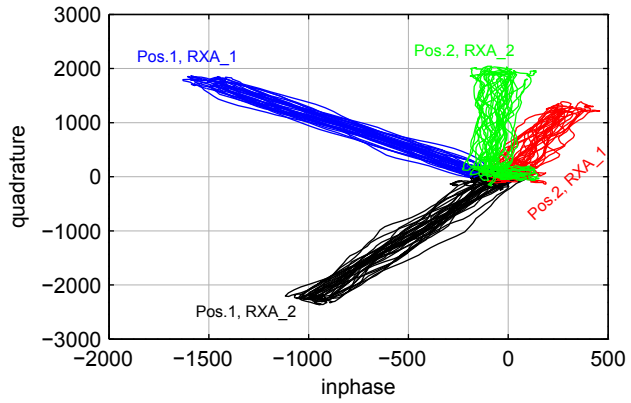


Fig. 8. Constellation diagrams of all four measurements with subtracted carrier in one scatter plot combined.

carriers from the four received constellations results in a shift of all constellations to the origin of the diagram. Fig. 8 shows now the different behavior of the two different positions Pos.1 and Pos.2 in amplitude as well as in different phase offsets at the receive antennas. The latter is caused directly by the different positions of the tags whereas the difference in amplitudes could also be a result of different backscatter efficiency of the tags used. Finally, the signal to noise ratios for the receive branches RXA_1, RX_1 and RXA_2, RX_2 and position Pos.1 are $\mathrm{SNR}_1 = 31.2\,\mathrm{dB}$ and $\mathrm{SNR}_2 = 32.4\,\mathrm{dB}$ and with position Pos.2 $\mathrm{SNR}_1 = 25.9\,\mathrm{dB}$ and $\mathrm{SNR}_2 = 30.2\,\mathrm{dB}$, respectively. For the second scenario an SNR improvement of 4.3 dB is possible with simple antenna selection. More sophisticated techniques as maximum ratio combining of course are enabled.

## V. Conclusion

The enhancement of current RFID systems using multiple antenna techniques as beamforming, diversity combining, or localization at the RFID reader also requires testing and measurement equipment which supports multiple transmitters and multiple receivers. The presented UHF frontend of our RFID rapid prototyping system supports two transmitters and two receivers and therefore enables novel experimental research in this field. As an example we presented a measurement with one transmitter and two receivers and two different tag positions. Transmit and receive beamforming as well as localization can be investigated based on the presented measurement results. Finally, the recorded data of the two receive branches can directly be used as a simulation input for designing multiple antenna receiver algorithms.

## References

[1] R. Want, "Enabling ubiquitous sensing with RFID," *Computer*, vol. 37, no. 4, pp. 84–86, April 2004.

[2] B. Nath, F. Reynolds, and R. Want, "RFID technology and applications," *IEEE Pervasive Computing*, vol. 5, no. 1, pp. 22–24, 2006.

[3] J. Griffin and G. Durgin, "Gains for RF tags using multiple antennas," *IEEE Transactions on Antennas and Propagation*, vol. 56, no. 2, pp. 563–570, Feb. 2008.

[4] A. Mindikoglu and A.-J. van der Veen, "Separation of overlapping RFID signals by antenna arrays," in *IEEE International Conference on Acoustics, Speech and Signal Processing, 2008. ICASSP 2008.*, 31 2008-April 4 2008, pp. 2737–2740.

[5] J. J. M. Wang, J. Winters, and R. Warner, "RFID system with an adaptive array antenna," US Patent, No. 7212116, May 2007.

[6] C. Angerer and R. Langwieser, "Flexible evaluation of RFID system parameters using rapid prototyping," in *IEEE International Conference on RFID*, Orlando, USA, April 2009.

[7] G. Meindl, R. Kloibhofer, F. Kaltenberger, and G. Humer, "Multi-standard development and measuring platform for MIMO-sofware definded radio," in *13th European Signal Processing Conference (EUSIPCO)*, Antalya, Turkey, September 2005.

[8] C. Angerer and M. Rupp, "Advanced synchronisation and decoding in RFID reader receivers," in *IEEE Radio and Wireless Symposium 2009*, San Diego, USA, January 2009.

[9] R. Langwieser, G. Lasser, C. Angerer, M. Rupp, and A. Scholtz, "A modular UHF reader frontend for a flexible RFID testbed," in *The 2nd Int. EURASIP Workshop on RFID Technology*, Budapest, Hungary, July 2008.